

## Intermittency and local dissipation scales under strong mean shear

Khandakar Niaz Morshed, Subhas Karan Venayagamoorthy, and Lakshmi Prasad Dasi

Citation: *Phys. Fluids* **25**, 011701 (2013); doi: 10.1063/1.4774039

View online: <http://dx.doi.org/10.1063/1.4774039>

View Table of Contents: <http://pof.aip.org/resource/1/PHFLE6/v25/i1>

Published by the AIP Publishing LLC.

---

### Additional information on Phys. Fluids

Journal Homepage: <http://pof.aip.org/>

Journal Information: [http://pof.aip.org/about/about\\_the\\_journal](http://pof.aip.org/about/about_the_journal)

Top downloads: [http://pof.aip.org/features/most\\_downloaded](http://pof.aip.org/features/most_downloaded)

Information for Authors: <http://pof.aip.org/authors>

### ADVERTISEMENT



**Running in Circles Looking  
for the Best Science Job?**

Search hundreds of exciting  
new jobs each month!

<http://careers.physicstoday.org/jobs>

physicstodayJOBS



## Intermittency and local dissipation scales under strong mean shear

Khandakar Niaz Morshed,<sup>1</sup> Subhas Karan Venayagamoorthy,<sup>2</sup>  
and Lakshmi Prasad Dasi<sup>1,a)</sup>

<sup>1</sup>Department of Mechanical Engineering, Colorado State University, Fort Collins, Colorado 80523, USA

<sup>2</sup>Department of Civil and Environmental Engineering, Colorado State University, Fort Collins, Colorado 80523, USA

(Received 8 October 2012; accepted 13 December 2012; published online 9 January 2013)

We experimentally probe the local dissipation scale distribution  $Q(\eta)$  and temporal fluctuations of the turbulent kinetic energy dissipation rate  $\epsilon$  in the strongly anisotropic flow past a backward facing step. A shift in  $Q(\eta)$  and corresponding reduction in the relative intermittency of  $\epsilon$  is observed with increasing mean shear  $S$ . We offer physical arguments to elucidate the role of strong shear on the small-scale structure. A local mean-shear dissipation Reynolds number,  $Re_S \equiv \langle \epsilon \rangle / (S^2 \nu)$ , is proposed that may define a family of universal small-scale structures of turbulence. © 2013 American Institute of Physics. [<http://dx.doi.org/10.1063/1.4774039>]

Intermittent spatio-temporal fluctuations of the instantaneous velocity gradient field are canonical to all turbulent flows. This translates to the highly intermittent spatio-temporal nature of the turbulent kinetic energy dissipation rate field  $\epsilon$ . Intermittency of energy dissipation rate can also be described in terms of a corresponding instantaneous fluctuating dissipation scale  $\eta$ . This fluctuating dissipation scale may be defined as  $\eta: Re_\eta = \eta \delta_\eta u / \nu \approx 1$ ; where  $\delta_\eta u = |u(x + \eta) - u(x)|$  is the longitudinal velocity increment.<sup>1,2</sup> Physically,  $\eta$  is the instantaneous cut-off scale where viscosity overwhelms inertia. Now, the notion of a fluctuating length scale  $\eta$  as the cut-off scale is different from the classical dissipative scale  $\eta_K = (\nu^3 / \langle \epsilon \rangle)^{1/4}$  proposed by Kolmogorov<sup>3</sup> in that it is defined over the instantaneous velocity field and thus directly relates to the governing equations. Nevertheless, the two paradigms to capture the dynamics of dissipative structures: (1) through a continuous distribution of dissipative scales represented by its probability density function (PDF)  $Q(\eta)$ , or (2) of a single dissipative scale  $\eta_K$ ; both predict a form of universal structure of turbulence at the small scales provided that the intermittency characteristics of  $\epsilon$  is universal (i.e., independent of the large scale). Equivalently, the small-scale structure of turbulence is universal if the distribution  $Q(\eta)$  has a form independent of the large scales. Identifying this universal form has been the quest of the statistical theory of turbulence for sufficiently large Reynolds numbers. Yakhot derived an analytical form for  $Q(\eta)$  by applying the Mellin transform properties to the structure function exponent relationships for moments of  $\delta_\eta u$ , combined with the Gaussian assumption.<sup>1</sup> This analytical estimate for high Reynolds number was constructed by utilizing an experimental fit to the measured behavior of the scaling exponent,  $\xi_n(n)$  in isotropic flows, where  $n$  is the order of the moment. Bailey *et al.* experimentally measured  $Q(\eta)$  in a turbulent pipe flow over a wide range of Reynolds numbers.<sup>4</sup> They concluded that  $Q(\eta)$  is indeed insensitive to local anisotropy for sufficiently high Reynolds numbers. Their result also suggested reasonable agreement with  $Q(\eta)$  calculated for the case of homogenous isotropic turbulence (HIT),<sup>5</sup> except as we argue that the slight deviation may have a significance. Most recently, Hamlington *et al.* performed direct numerical simulations (DNS) of the wall bounded turbulent shear flow<sup>6</sup> as a stronger test of universality of  $Q(\eta)$ . They studied

<sup>a)</sup> Author to whom correspondence should be addressed. Dr. Lakshmi Prasad Dasi, 1374 Campus Delivery, Department of Mechanical Engineering, Colorado State University, Fort Collins, CO 80523. E-mail: [lakshmi.dasi@colostate.edu](mailto:lakshmi.dasi@colostate.edu).

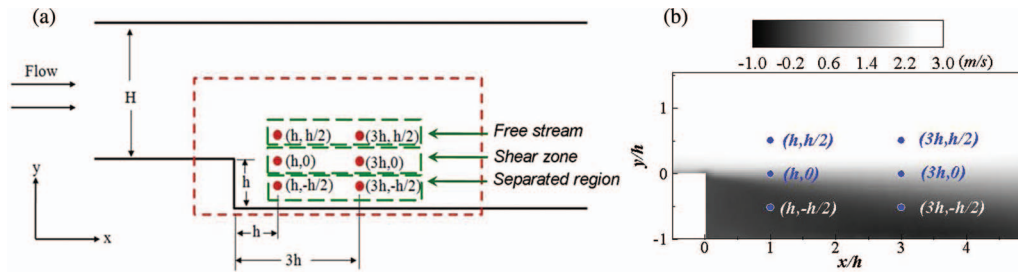


FIG. 1. Sketch of the backward facing step (a) and mean streamwise velocity contours (b). Dashed box indicates the measurement region for particle image velocimetry. Six positions corresponding to the locations with varying large-scale anisotropy have been highlighted in the sketch as well as in the mean velocity contour plot.

the distribution of  $Q(\eta)$  at varying  $y^+$  locations and varying Reynolds numbers. They found that at lower  $y^+$  the peak of  $Q(\eta/\eta_0)$  significantly shifts along the  $\eta/\eta_0$  axis, where  $\eta_0 = L Re_L^{-0.72}$  ( $L$  being the local integral length scale,  $Re_L = k^{1/2}L/\nu$ , and  $k$  the local turbulent kinetic energy). Although for  $y^+ > 90$ , their results are in good agreement with that corresponding to pipe flows<sup>4</sup> and HIT,<sup>5</sup> there are significant departures for  $y^+ < 90$ , which includes a portion of the log-layer and the buffer layer. This departure was attributed to the specific properties of near wall coherent structures. In this letter, we explore if the anisotropic behavior of  $Q(\eta/\eta_0)$  for  $y^+ < 90$  is a more general property of turbulent flows in the presence of strong mean shear. To test this, we performed a high resolution experiment to examine both the fluctuations in the dissipation rate as well as  $Q(\eta/\eta_0)$  within and around the strong free shear flow downstream of the flow past a backward facing step. The backward facing step flow is an anisotropic turbulent flow with a strong free shear region presumably void of the peculiar characteristics of coherent structures found in the near wall channel flow turbulence. As reported in the remainder of this letter, we report that the departure from isotropic behavior previously found in the near wall region in fact points to a more general mechanism linked to the presence of locally strong mean shear. Based on these observations, we propose that a family of universal forms for  $Q(\eta/\eta_0)$  must exist and can be parameterized by a local mean shear-dissipation Reynolds number defined as  $\langle \epsilon \rangle / (S^2 \nu)$ . We offer physical reasoning to support this argument.

High-resolution, two-dimensional, time-resolved particle image velocimetry (PIV) experiments were carried out to capture the turbulent velocity field along the centerline of a rectangular channel flow with a backward facing step. A sketch of the backward facing step is shown in Figure 1 along with a contour plot of the ensemble averaged mean streamwise velocity. The step size  $h$  was 5 mm with the channel length being  $172h$ . The inlet and outlet cross sections of the rectangular channel were roughly  $6h \times 13h$  and  $7h \times 13h$ , respectively. The expansion ratio defined as  $(H + h)/H$ , was 1.172 with an aspect ratio of  $b/H = 2.24$ , where  $b$  is the channel width and  $H$  the channel height. Water at room temperature was circulated through the acrylic channel driven by a submersible pump in a closed loop manner. The Reynolds number  $Re_h$  was 13,600 based on the maximum free-stream velocity  $U_0$  and step height  $h$ ;  $Re_D$  was 108,800, based on inlet hydraulic diameter. Raw PIV images were pre-conditioned prior to vector calculations by subtracting a sliding background image. Particle intensity normalization was done using a max/min filter, which helped to obtain homogeneous particle intensities. The measurement region captured the instantaneous turbulent 2D velocity field in the streamwise ( $x$ )  $\times$  wall normal ( $y$ ) directions along the channel centerline immediately downstream of the step. The velocity field sampling rate was 2 kHz and the spatial resolution of the data was  $27.8 \mu\text{m}$ , which was confirmed to satisfy the condition in Ref. 7 to reasonably estimate  $\epsilon$ . The total number of ensembles obtained was 4,215. Within the measurement domain, six positions of interrogation were chosen such that two were within the intense shear layer, two above in the free stream, and two below in the separated region (see Figure 1). With the origin being the corner of the step, the interrogation positions were  $(h, h/2)$  and  $(3h, h/2)$  in the free stream;  $(h, 0)$  and  $(3h, 0)$  in the strong shear layer; and  $(h, -h/2)$  and  $(3h, -h/2)$  within the separated zone, respectively. These points of interest correspond to regions of varying characteristics of the large scale anisotropy, particularly the magnitude of the principal mean shear rate,  $S$ . The principal mean

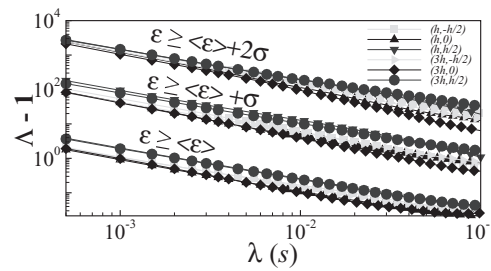


FIG. 2. Lacunarity of the instantaneous dissipation rate signal measured at each of the six positions downstream of the backward step for three threshold levels. The data corresponding to thresholds of 1 and 2 standard deviations above the mean have been shifted up by 1 and 2 decades, respectively.

shear rate at each of the positions in (1/s) were 1730.2 ( $h, 0$ ); 1302.4 ( $3h, 0$ ); 286.57 ( $h, h/2$ ); 212.7 ( $3h, h/2$ ); 272.3 ( $h, -h/2$ ); and 770.1 ( $3h, -h/2$ ).

We calculated the lacunarity of the instantaneous dissipation rate signals at the six interrogation points. Instantaneous  $\epsilon$  was calculated using the two-dimensional surrogate approach described in Ref. 7 as  $\epsilon = (3\nu(s_{11}^2 + s_{22}^2) + 12\nu s_{12}^2)$ , with the isotropic assumptions  $\langle s_{13}^2 \rangle = \langle s_{23}^2 \rangle = \langle s_{12}^2 \rangle$ , and  $\langle s_{33}^2 \rangle = 0.5(\langle s_{11}^2 \rangle + \langle s_{22}^2 \rangle)$ . Lacunarity is a fractal measure that characterizes the temporal homogeneity in a multi-fractal signal. It is particularly sensitive to the pattern of intermittent signal bursts occurring at varying time scales, see Refs. 8 and 9. First, the raw dissipation signal is converted into a binary signal via a pre-set threshold. Given a window size (time scale)  $\lambda$ , the mass signal is obtained as the integral of the binary signal within the window. As the window slides across the entire time-series, the mass signal fluctuates. Lacunarity  $\Lambda(\lambda)$  is then evaluated as  $\Lambda(\lambda) = 1 + (\sigma_m^2)/(\mu_m^2)$ , where  $\sigma_m^2$  is the variance and  $\mu_m^2$  is the square of the averaged mass signal time-series. Physically,  $\Lambda(\lambda)$  reflects the level of inhomogeneity and intermittency in the signal. Figure 2 shows the lacunarity of  $\epsilon$  for three different thresholds namely,  $\langle \epsilon \rangle$ ,  $\langle \epsilon \rangle + \sigma$ , and  $\langle \epsilon \rangle + 2\sigma$  for each of the six locations, where  $\sigma$  is the standard deviation of the fluctuating  $\epsilon$ . The lacunarity functions have been shifted up by one decade for  $\langle \epsilon \rangle + \sigma$  and two decades up for  $\langle \epsilon \rangle + 2\sigma$ . The graphs show that the dissipation rate lacunarity for locations ( $h, 0$ ) and ( $3h, 0$ ) is consistently lower than at other locations which have lower local mean shear. Lower lacunarity implies that the mass signal fluctuates less relative to its mean. This translates to smaller but more frequent bursts in the dissipation rate signal. This is in stark contrast with the large but not so frequent bursts measured at the low mean shear locations. Notice how this is true at all time scales,  $\lambda$ . The above fractal analysis shows a measurable shift in the geometric properties of the dissipation rate signal with increasing shear. Gaps between bursts are smaller with increasing shear and the bursts are not so large relative to the mean (although the average dissipation rate is higher). Strikingly, these are the same conclusions from the dissipation statistics analyzed within the strong shear dominated near wall region in Ref. 10.

PDFs of the local dissipation scale,  $Q(\eta)$  was calculated for each of the six interrogation points. The approach is identical to that described in Refs. 4, 6, and 11 with the qualifying condition for  $\eta$  being  $0.9 \leq \eta \delta_\eta u / \nu \leq 2$ . Only longitudinal increments were considered.  $\eta$  was normalized with  $\eta_0 = L Re_L^{-0.72}$ ; where  $L$  is the integral length scale and  $Re_L = L \langle \delta_L u^2 \rangle^{1/2} / \nu$ . Figure 3(a) shows  $Q(\eta/\eta_0)$  for the six locations along with previously published results of Refs. 4, 5, and 6. From the figure, it is clear that the peak location for ( $h, 0$ ) and ( $3h, 0$ ) in the intense shear layer significantly shifts to values higher than that for the case of HIT (shown more clearly in Figure 3(b)). The location of the peak appears similar to those in Ref. 6 for  $30 < y^+ < 90$  at  $Re_\tau = 590$ . To confirm that these shifts are indeed significant, we calculated the uncertainty in the PDFs. Given that the PDF is derived from the histogram of the occurrence of  $\eta$ , and that the measured variable in the above inequality is  $\delta_\eta u$ , it is straight forward to propagate the percent error in the instantaneous velocity of the PIV measurements to the uncertainty in the PDF. Our uncertainty of 2.5% in velocity translates to an uncertainty of 2.8% in  $\delta_\eta u$ . Given that the inequality is the only qualifying criteria, the uncertainty in the PDF may be achieved by perturbing the upper and lower limits of the inequality. To be conservative, we recalculated the PDFs by incorporating a 10% variation in the limits and found that the resulting PDFs with this additional 10% uncertainty in  $\delta_\eta u$  insignificantly influenced the

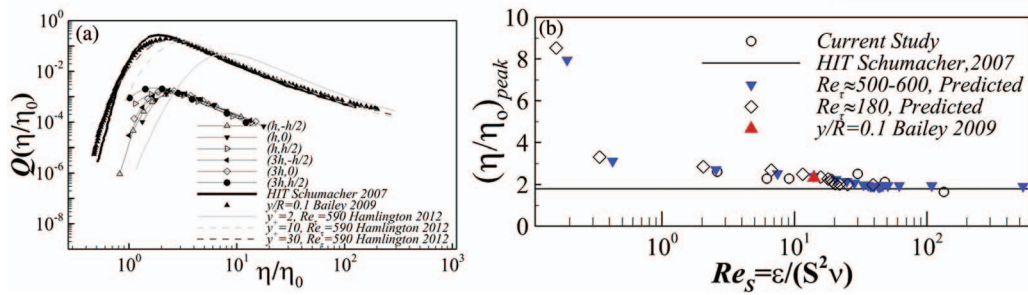


FIG. 3. Local dissipation scale PDF  $Q(\eta/\eta_0)$  measured at each of the six positions downstream of the backward step (a). Data points have been shifted down by 2 decades to aid comparison with previously reported  $Q(\eta/\eta_0)$  in HIT,<sup>5</sup> and wall bounded flows.<sup>4,6</sup>  $(\eta/\eta_0)_{peak}$  plotted as a function of  $Re_S$  for each of the six positions downstream of the backward step (b). This is being compared to the corresponding relationship in channel flows at two different Reynolds numbers.  $(\eta/\eta_0)_{peak}$  for HIT,<sup>5</sup> and pipe flow  $y/R = 0.1$  (Ref. 4) are depicted as constant levels.

shape and position of the peak (same histogram bin with maximum counts). The error in  $\eta_0$  was estimated at 2.5% based on statistical convergence. Thus, the overall error in the normalized peak location is roughly 2.5%. As seen in both Figures 2 and 3, the intermittent fluctuations of  $\epsilon$  and the corresponding distribution of  $\eta$  is clearly dependent on the strong mean shear. While this does not debunk the notion of universality of small-scale turbulent fluctuations, it does indicate the need to refine the description of the small-scale structure by including local anisotropy parameters to further refine the theoretical model of the distribution of  $\eta$ . In this direction, here we provide dimensional arguments to elucidate how strong mean shear can physically alter the small scale structure. Given that mean shear,  $S$  regulates turbulence production; it must define a range of production length scales that represent the injection of turbulent kinetic energy or stirring. These production length scales ranging from the large scale to the smallest scale may be defined as

$$L_{S,\epsilon} = (\langle\epsilon\rangle/S^3)^{1/2}; \text{ and } L_{S,\nu} = (\nu/S)^{1/2}. \quad (1)$$

While  $(\langle\epsilon\rangle/S^3)^{1/2}$  is a turbulent length scale, which phenomenologically represents the cut-off representing the dominance of mean shear driven energy production as opposed to the transfer via the energy cascade,  $(\nu/S)^{1/2}$  is not. Physically, given a stationary mean shear flow,  $(\nu/S)^{1/2}$  gauges the size of a ball surrounding a point in the fluid domain whose Reynolds number is one. Thus, it is the dissipative scale, similar to the definition of  $\eta$ , but of the mean flow. Another physical interpretation is that it is the length scale across which the turbulent dissipation rate at that length scale  $\sim \nu^3/L_{S,\nu}^4$  is equal to the viscous dissipation rate of the smooth mean flow,  $\sim \nu S^2$ .

It is evident from these dimensional constructions that the above shear derived scales tend to infinity as  $S \rightarrow 0$ , indicating that production at low shear occurs at the large scale. It also indicates that as the local shear magnitude increases, both  $(\langle\epsilon\rangle/S^3)^{1/2}$  and  $(\nu/S)^{1/2}$  can begin to overlap with the range of the fluctuating  $\eta$ . Notice that the ratio of the squares of  $(\langle\epsilon\rangle/S^3)^{1/2}$  to  $(\nu/S)^{1/2}$  defines the mean shear-dissipation Reynolds number  $Re_S$  given by

$$Re_S = \langle\epsilon\rangle/(S^2\nu), \quad (2)$$

which  $\rightarrow 0$  with increasing magnitude of  $S$ . It is also easy to see that the ratio of  $(\langle\epsilon\rangle/S^3)^{1/2}$  to the Kolmogorov scale is  $Re_S^{3/4}$ . Furthermore,  $Re_S$  can be either expressed in terms of the turbulence Reynolds number as  $Re_S = Re_L(ST_L)^{-2}$ , where  $T_L = k/\epsilon$  is the turbulence time scale, or in terms of the Kolmogorov time scale as  $Re_S = (S\tau_\eta)^{-2}$ , where  $\tau_\eta$  is the Kolmogorov time scale  $(\nu/\epsilon)^{1/2}$ . The dimensionless time-scale ratio  $ST_L$  thus emerges as being truly independent. Given that the presence of mean shear adds an independent dimension to the dimensionless formulation of scales; the influence of mean shear may be hypothesized as (1) shear flow turbulence can have the same structure and dynamics as isotropic turbulence provided both  $Re_L$  and  $Re_S$  are large (i.e., when  $ST_L \rightarrow 0$ ); (2) for large  $Re_L$  but  $Re_S$  of  $O(1)$  (i.e.,  $ST_L \gg 0$ ), the structure of turbulence significantly departs from the isotropic picture; and finally (3) there exists a family of universal structure of small-scale turbulence defined by the parameter  $Re_S$  or more independently by  $ST_L$  for

very large  $Re_L$ . Hypotheses (1) and (2) were in fact anticipated by Corrsin<sup>12</sup> who argued on the basis of competition between the local energy transfer time scale and the normalized mean shear time scale captured by  $S\tau_\eta$ . We also note here that the above dimensional arguments can also be formulated on the fluctuating turbulent velocity field. It is easy to see that  $Re_S$  can be expressed in terms of the fluctuating dissipation scale  $\eta$  as  $Re_S \sim \langle (S\eta^2/\nu)^{-2} \rangle$ . Thus, one may pose the same arguments as above without invoking dimensional analysis, by defining an alternative shear-dissipation scale Reynolds number as a moment defined over  $Q(\eta)$  given by  $\int_0^L (S\eta^2/\nu)Q(\eta)d\eta$ . Thus, the local dissipation dynamics departs from the isotropic expectation if instantaneously the number  $S\eta^2/\nu \gg 1$ . Physically, this represents the cut-off where locally  $S\eta \gg \delta_\eta u$ . With regards to hypothesis (3), it indicates the possible existence of a more general universality class for the small-scale structure of turbulence that is applicable for all shear flows as long as the mechanism of turbulence production is purely shear driven, and that the classical picture is only a special case when shear vanishes. Now, the existence of a universal structure that is shear dependent may sound like an oxymoron given that mean shear has classically been associated with the large scale. But it could be true if and only if the very mechanism of shear driven turbulence production itself were to be universal. In other words, the turbulent production mechanisms in the strong shear region of a free jet is statistically identical to turbulent production in a mixing layer or even a boundary layer provided the relevant dimensionless numbers (i.e.,  $Re_L$  and  $Re_S$  as suggested above) are matched. Combining this notion of a universal turbulence production structure with the underlying universal multi-fractal structure, the nature of the small-scale structure is hypothesized to obey a new class of universality that is dependent on precisely the relative position of the production scales (defined by  $Re_S$ ) with respect to the separation of turbulent scales. These ideas extend the classical notion of universality, which still hold as a special case at vanishing shear and, as discussed in the context of the data presented in the remainder of this letter, remains to be a very good approximation for  $Re_S \geq 40$ .

Using our data and previously published data, we performed a preliminary test for hypothesis (1) through (3). This was done by recasting both our data and the shear flow data from Refs. 4 and 6 to analyze the departure of  $Q(\eta/\eta_0)$  from the HIT expectation as a function of  $Re_S$ . Figure 3(b) shows a plot of the peak location of  $Q(\eta/\eta_0)$ ,  $(\eta/\eta_0)_{peak}$  as a function of  $Re_S$  for the six locations. The figure also shows the predicted curves for turbulent channel flows for  $Re_\tau \sim 550$  and  $Re_\tau \sim 180$ . These predictions were based on  $(\eta/\eta_0)_{peak}$  presented in Ref. 6 combined with  $\langle (\epsilon) \rangle / (S^2\nu)$  calculated from the freely distributed channel flow data of Ref. 13. Pipe flow data at  $y/R = 0.1$  in Ref. 4 is also included, along with the level corresponding to HIT. It is clear from this composite data-set that at large  $Re_S$ ,  $(\eta/\eta_0)_{peak}$  approaches the HIT level, partially supporting hypothesis (1). The data also show a significant departure for  $Re_S < 40$  with  $(\eta/\eta_0)_{peak}$  increasing in magnitude. There appears to be an inflection for  $Re_S \sim 1$  and a rapid increase in  $(\eta/\eta_0)_{peak}$  for  $Re_S < 1$ . The significant deviation from HIT for  $Re_S < 40$  supports hypothesis (2). All the data show reasonable collapse. The significantly higher  $(\eta/\eta_0)_{peak}$  for  $Re_S \sim 30$  in the PIV data was examined closer, and can be explained through the inherent limitation of defining the integral length scale in strongly anisotropic flows (which is the next challenge to address before testing these hypothesis in much stronger anisotropic flows). This data point corresponds to location  $(h, -h/2)$ , which lies within the separated zone. The point is within 0.3 mm of the strong shear layer and thus, the longitudinal two-point correlation function inevitably traverses from low to high shear. We would like to note that if we recalculate the position of this data point by revising the mean shear at this location as the average over the integral length scale, the data point shifts to the left and exactly falls in line further improving the collapse of data. We also note here that the  $(\eta/\eta_0)_{peak}$  level corresponding to pipe data at  $y/R = 0.1$  (Ref. 4) agrees more with the collapsed data than the HIT prediction. All of these observations with a reasonable data collapse seem to support hypothesis (3) with respect to the existence of a family of universal structures of turbulence. However, more studies are necessary to study this behavior in multi-directional anisotropy with a more general definition of integral length scale. To illustrate how  $Re_S$  significantly varies in space and can therefore play a significant role in the variation in local structures, Figure 4 shows profiles of  $Re_S$  as a function of  $y/h$  at  $x \approx h$  and  $x \approx 3h$ . From this figure, it is clear that the shear layer indeed significantly reduces  $Re_S$  particularly along  $y/h = 0$ . The inset shows profiles of  $Re_S$  as a function of  $y^+$  in channel flows based on Ref. 13 for very high  $Re_\tau$ . This figure clearly shows that roughly at  $y^+ \sim 90$ ,  $Re_S \sim 40$ . This further explains the

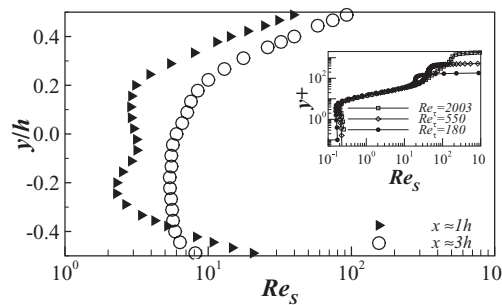


FIG. 4. Profiles of  $Re_s$  along the wall normal direction  $y/h$  at two distances downstream of the backward step. Inset shows the corresponding profile along the wall normal direction  $y^+$  derived from channel flow DNS simulations<sup>13</sup> at three Reynolds numbers.

departure of  $Q(\eta/\eta_0)$  from the HIT behavior for  $y^+ < 90$ .<sup>6</sup> It also explains the departure observed in our data for regions with large mean shear in the free shear layer downstream of the backward step.

In summary, this letter has shown the relevance of considering local anisotropic parameters such as the mean shear in tackling the problem of understanding the departure of small-scale structure of turbulence in strongly anisotropic yet high Reynolds number flows from that observed for the case of HIT. Through physical arguments, we have proposed that there may exist a family of universal structures of turbulence through the introduction of the mean shear Reynolds number  $Re_s$  or equivalently the ratio of mean shear time scale to turbulence time scale  $ST_L$ . Alternatively, it can also be described by the Reynolds number  $\int_0^L (S\eta^2/\nu)Q(\eta)d\eta$ . Our high-resolution PIV measurements in the backward facing step not only shows that the fluctuation in dissipation rate becomes relatively less intermittent in the presence of strong shear (through fractal analysis), but also that the peak location of  $Q(\eta/\eta_0)$  shifts to the right. This shift is consistent with near wall  $Q(\eta/\eta_0)$  in channel flows where mean shear is high. By combining our data and performing meta-analysis of previous data in channel flow turbulence, we have shown that  $Re_s < 40$  significantly marks the shift for the small scale structure from HIT behavior. We have shown partial evidence that this shift may still be universal as our data, which consist of free-shear turbulence, agree with the wall-bounded turbulence and HIT when parameterized with  $Re_s$ . However, further detailed investigations of increasingly complex anisotropic turbulent flows, with strong principal shear as well as a generalized definition of integral length scale independent of the two-point correlation function, are needed.

<sup>1</sup> V. Yakhot, "Probability densities in strong turbulence," *Physica D* **215**, 166 (2006).

<sup>2</sup> V. Yakhot and K. R. Sreenivasan, "Anomalous scaling of structure functions and dynamic constraints on turbulence simulations," *J. Stat. Phys.* **121**, 823 (2005).

<sup>3</sup> A. Kolmogorov, "The local structure of turbulence in incompressible viscous fluids at very large Reynolds numbers," *Dokl. Akad. Nauk SSSR* **30**, 299–303 (1941).

<sup>4</sup> S. Bailey, M. Hultmark, J. Schumacher, V. Yakhot, and A. Smits, "Measurement of local dissipation scales in turbulent pipe flow," *Phys. Rev. Lett.* **103**, 014502 (2009); e-print [arXiv:0906.1116](https://arxiv.org/abs/0906.1116).

<sup>5</sup> J. Schumacher, "Sub-Kolmogorov-scale fluctuations in fluid turbulence," *EPL* **80**, 54001 (2007).

<sup>6</sup> P. E. Hamlington, D. Krasnov, T. Boeck, and J. Schumacher, "Local dissipation scales and energy dissipation-rate moments in channel flow," *J. Fluid Mech.* **701**, 419 (2012).

<sup>7</sup> T. Tanaka and J. K. Eaton, "A correction method for measuring turbulence kinetic energy dissipation rate by PIV," *Exp. Fluids* **42**, 893 (2007).

<sup>8</sup> R. Plotnick, R. Gardner, W. Hargrove, K. Prestegard, and M. Perlmutter, "Lacunarity analysis: A general technique for the analysis of spatial patterns," *Phys. Rev. E* **53**, 5461 (1996).

<sup>9</sup> L. P. Dasi, F. Schuerg, and D. R. Webster, "The geometric properties of high-Schmidt-number passive scalar iso-surfaces in turbulent boundary layers," *J. Fluid Mech.* **588**, 253 (2007).

<sup>10</sup> P. E. Hamlington, D. Krasnov, T. Boeck, and J. Schumacher, "Statistics of the energy dissipation rate and local enstrophy in turbulent channel flow," *Physica D* **241**, 169 (2012).

<sup>11</sup> Q. Zhou and K.-Q. Xia, "Universality of local dissipation scales in buoyancy-driven turbulence," *Phys. Rev. Lett.* **104**, 104301 (2010).

<sup>12</sup> S. Corrsin, "Local isotropy in turbulent shear flow," National Advisory Committee for Aeronautics Research Memorandum **58B11**, 1 (1958).

<sup>13</sup> S. Hoyas and J. Jimenez, "Reynolds number effects on the Reynolds-stress budgets in turbulent channels," *Phys. Fluids* **20**, 101511 (2008).